FLOW STRUCTURES AND HEAT TRANSFER ON DIMPLED SURFACES

Johann Turnow, Valery Zhdanov, Egon Hassel
Institute of Technical Thermodynamics
University of Rostock
Albert-Einstein-Str. 2, 18059 Rostock
johann.turnow@uni-rostock.de

Nikolai Kornev
Institute of Modeling and Simulation
University of Rostock
Albert-Einstein-Str. 2, 18059 Rostock
nikolai.kornev@uni-rostock.de

ABSTRACT

Vortex structures and heat transfer enhancement mechanism in a turbulent flow over a staggered dimple array in a narrow channel have been investigated using Large Eddy Simulation (LES), Laser Doppler Velocimetry (LDV) and pressure measurements for $\mathrm{Re}_D = 10000$ and $\mathrm{Re}_D = 20000$. The flow and temperature fields are captured by LES using dynamic mixed model applied both for the velocity and temperature. Simulations are validated by comparison with experimental data obtained for smooth and dimpled channels. Experiments and LES show that the time averaged fields are symmetric in spanwise direction for each dimple. The flow inside of the dimple is chaotic and consists of small eddies with a broad range of scales where coherent structures are hardly to detect. For both Reynolds numbers it was found that the dimple package with the depth t to diameter D ratio of $t/D = 0.26$ provides the highest heat transfer and thermo-hydraulic performance. Proper Orthogonal Decomposition (POD) method is applied to resolved LES fields to identify spatial-temporal structures hidden in the random fluctuations of pressure and velocity fields.

INTRODUCTION

At present several methods of heat transfer enhancement like ribs, fins or dimples have been thoroughly investigated with the aim to improve the heat exchange at a minimum hydraulic loss. It has been shown by many authors (see Ligrani P.M. (2003)) that concave formed dimples in comparison to other conventional methods show the best thermo-hydraulic performance defined as the ratio between the heat exchange and the pressure loss increases. Depending on the dimple/channel configuration and on the flow properties, the spatially averaged Nusselt number Nu referred to that of a smooth channel Nu_0 varies from $Nu/Nu_0 = 1.1$ to $Nu/Nu_0 = 2.5$. The relative pressure resistance increase varies in a range of $C_p/C_{p0} = 1.05 - 3.5$ which is fairly low compared to other methods.

High values of the thermo-hydraulic performance $Nu/Nu_0/(C_p/C_{p0})^{1/3}$ are attained on dimples because of an efficient way of vortex generation. The vortices on ribs and fins, which are necessary to mix the fluid, are created through the flow separation on protruding elements what results in a high pressure drag. The vortices on dimpled surfaces are created inside of concave cavities. Since there is no blockage of the channel the additional resistance is minimum. Because the vortices play a significant role in the convection enhancement, their formation was in the focus of many studies. Unfortunately, in most investigations main attention is paid to time averaged values whereas the flow structures within the cavities and their contribution to the heat transfer mechanism remain still unclear and are not completely understood.

The most detailed experimental study of unsteady flow characteristics on dimpled packages has been performed by Ligrani P.M. (2003). Flow visualization by smoke patterns revealed a primary vortex pair and additionally two secondary vortices arise at the spanwise edges of each dimple which enhance mixing process. Unfortunately, these first valuable observations of an array of dimples have never been quantified properly and analyzed using modern non-intrusive measurement techniques and advanced numerical technologies like LES and DNS.

The objective of this investigation is to clarify the role of the vortex formations with respect to the heat transfer on staggered dimple packages using LES and time resolved pressure and velocity measurements. In our previous work Turnow J. (2010) vortex structures have already been investigated for a single spherical dimple. LES simulations revealed formation of asymmetric structures with an orientation switching between two extreme positions. The emphasis of the present work is identification of vortex structures on dimple packages. Since the augmentation of heat transfer is documented for dimples with a depth to diameter ratio of $t/D \geq 0.22$ the

range of t/D between 0.195 and 0.326 is investigated at turbulent flow regimes at $\mathrm{Re}_D = 10000$ and $\mathrm{Re}_D = 20000$.

EXPERIMENTAL SETUP

Experimental investigations have been performed in a closed water loop channel schematically presented in Figure 1. Main parts of the test rig are the head tank with an overflow weir inside, a settling chamber, the converging nozzle (contraction) followed by the test section and a back tank with a metering system. Further a water reservoir, main pump, pipelines and four controlling valves are placed between each device to ensure stable water levels. Water is pumped from the reservoir into the head tank by the main pump which can be additionally tuned to control the mass flow rate. Insight the main tank a weir is installed to reduce turbulence caused by the water pump. In addition an overflow pipe is placed at a predefined height into the head tank to provide a constant water level. The advantage of this set-up construction is that a constant water level is ensured in the head tank providing flow with a constant flow rate and a low level of turbulence inside the test section. The rectangular test channel section behind the converging nozzle has the dimension in terms of channel width B, channel height H and total length L of $200mm \times 15mm \times 1340mm$. To provide visual access the test section was made of acrylic glass. Thirty rows of dimples with a print diameter of $D = 23mm$ and depth of $t = 6mm$ were drilled in a staggered arrangement and then polished by a CNC machine on the lower channel wall. The first row was placed at $500mm$ behind the inlet of the test section (see Figure 2). To measure the static pressure loss, twelve bore holes with an inner diameter of 1.5 mm were drilled along the centerline of the test section. The pressure resistance coefficient C_p for both smooth and dimpled channels is calculated as the pressure difference between the inlet and outlet of the dimple package.

LARGE EDDY SIMULATION

Large Eddy Simulations (LES) have been performed based on a 3-D finite volume method. The filtered transport equations are solved on a non staggered Cartesian grid, the discretisation in space and time of the quantities at the cell faces is of second order using central differencing scheme. The LES equations are obtained by filtering the continuity equation, the Navier-Stokes equations and the transport equation for the nondimensional temperature θ at the filter width $\widetilde{\Delta}$:

$$\frac{\partial \widetilde{u}_i}{\partial t} + \frac{\partial \widetilde{u}_j \widetilde{u}_i}{\partial x_j} = -\frac{1}{\rho}\frac{\partial \widetilde{P}}{\partial x_i} + \frac{\partial}{\partial x_j}\left[\nu\left(\frac{\partial \widetilde{u}_i}{\partial x_j} + \frac{\partial \widetilde{u}_j}{\partial x_i}\right) - \tau_{ij}\right], \tag{1}$$

$$\frac{\partial \widetilde{\theta}}{\partial t} + \frac{\partial \widetilde{u}_j \widetilde{\theta}}{\partial x_j} = \frac{\partial}{\partial x_j}\left[\frac{\nu}{\mathrm{Pr}}\frac{\partial \widetilde{\theta}}{\partial x_j} - J_j^{SGS}\right]. \tag{2}$$

The unclosed subgrid stress tensor $\tau_{ij} = \widetilde{u_i u_j} - \widetilde{u}_i \widetilde{u}_j$ and the subgrid contribution to the scalar dynamics $J_j^{SGS} = \widetilde{\theta u_j} - \widetilde{\theta}\widetilde{u}_j$ are modeled in terms of the filtered quantities $\widetilde{u}_i$ and $\widetilde{\theta}$,using the localized dynamic mixed model (LDMM) (Zang, 1993). In Eq. 2 the non-dimensional temperature θ is defined as $(\theta = (T - T_{lowerwall})/(T_{lowerwall} - T_{upperwall}))$ and further treated as a passive scalar without buoyancy effects. The molecular Prandtl number Pr was set to $\mathrm{Pr} = 0.7$, whereas in LES the turbulent viscosity μ_t and the turbulent Prandtl number Pr_t are determined dynamically using LDMM. To ensure the numerical stability of the DMM a clipping procedure derived from a rigorous mathematical analysis based on Taylor series approximation is applied (see Kornev (2007)).

Since the whole dimple package starting from the first row can not be simulated by LES due restricted computer resources only a part of dimples located within the full developed flow was considered (see Figure 2). It should be noted that the domain size should be chosen carefully to capture typical velocity and temperature structures. In the most of previous works time resolved calculations of heat exchangers with dimples or protrusions have been performed for a half or for only one whole dimple with enforced periodic conditions in streamwise and spanwise directions. This domain size is not sufficient because the typical vortex structures can be larger than the dimple diameter. In this work a large domain with the dimension $4.66H \times H \times 4.66H$, where H is the channel height, including several dimples was chosen to guarantee capturing largest flow structures. The diameter D of the dimple with a sharp edge was kept constant at $D = 23$ mm. Three different dimple depths t of $t/D = 0.196$, $t/D = 0.26$ and $t/D = 0.326$ were studied. Periodic boundary conditions were applied in streamwise and spanwise directions. No slip wall condition were enforced on the lower and the upper solid walls for the velocity and fixed values were set for the temperature at the lower (hot surface, $\theta = 1$) and the upper (cold surface, $\theta = 0$) channel wall. To drive the flow with a constant massflow rate the overall losses are calculated within the domain and simply added as the driving force to the momentum equation.

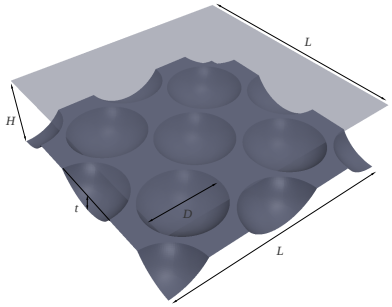

Figure 2: Computational domain of the channel with dimples at the lower wall

RESULTS

Validation

For validation, reference and for establishment of the grid independency a series of calculations of a turbulent channel flow with the dimension of $4.66H \times H \times 4.66H$ with

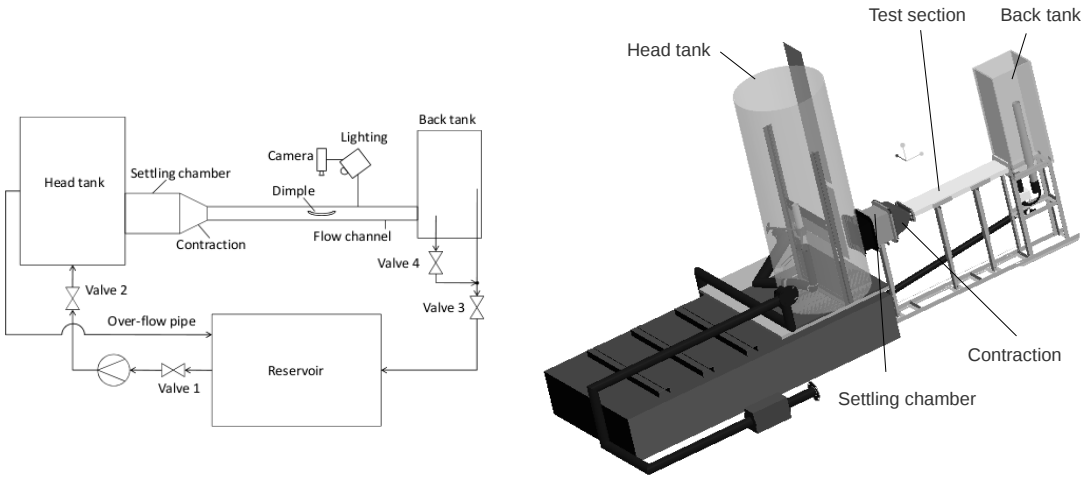

Figure 1: Flow chart and sketch of the experimental bench

smooth walls have been carried out first. Two Reynolds numbers $\mathrm{Re}_D = U_{bulk}D/\nu = 10000$ and $\mathrm{Re}_D = 20000$ were considered which are equivalent to the Reynolds numbers $\mathrm{Re}_H = U_{bulk}H/\nu = 6521$ and $\mathrm{Re}_H = 13042$ based on the channel height H. The total number of grid points used for the channel flow is $256 \times 80 \times 256 \approx 5.25 \cdot 10^6$. In spanwise and streamwise direction homogeneous grid stretching is used normal to the wall with the first grid point is placed at $y^+ = 0.4$. Table 1 summarizes the results for the skin-friction coefficient C_f obtained from numerical simulation and our pressure measurements. The skin-friction coefficients obtained from ex-

Table 1: Comparison of the skin-friction coefficient C_f obtained from LES and experiment with empiric correlations from Dean for a turbulent channel flow at $\mathrm{Re}_H = 6521$ and $\mathrm{Re}_H = 13042$.

		C_f	Dean
$\mathrm{Re}_H = 6521$	LES	0.0671	0.06835
	Exp	0.0692	
$\mathrm{Re}_H = 13042$	LES	0.0591	0.05748
	Exp	0.0602	

periment and simulations show very good agreement with the empirical correlation given by Dean $C_f = 0.06138\ \mathrm{Re}^{-1/4}$. Comparison of LES data for the heat transfer rates with the empiric correlations of Gnielinsky

$$Nu = \frac{(\xi/8)\ \mathrm{RePr}}{1 + 12.7\sqrt{\xi/8}\ (\mathrm{Pr}^{2/3} - 1)}(1 + (d_h/l)^{2/3}) \quad (3)$$

and Dittuis-Boelter $Nu = 0.023\ \mathrm{Re}^{0.8}\ \mathrm{Pr}^{0.4}$ is summarized in Table 2. The discrepancy does not exceed 1% what under-

Table 2: Comparison of Nusselt number Nu of LES and empiric correlations from Gnielinsky and Dittuis-Boelter for a turbulent channel flow at $\mathrm{Re}_H = 6521$ and $\mathrm{Re}_H = 13042$.

		Nu	Boelter	Gnielinsky
$\mathrm{Re}_H = 6521$	LES	23.78	22.39	24.04
$\mathrm{Re}_H = 13042$	LES	38.4	38.97	38.87

lines the accuracy of the present calculations. On the basis of the turbulent channel flow calculations, a block structured curvilinear grid consisting of 13'196'000 cells was chosen for further investigations of the dimpled channel shown in Figure 2. To escape numerical errors caused by large aspect ratios of grid cells, mesh motion functionality based on a grid diffusion equation was applied. At the first step a block-structured grid is generated for flat channel and then a mesh diffusion was used to stretch the mesh onto the dimpled surface. As a result, the grid lines nearly follow the streamlines inside the dimples and large aspect ratios are avoided. Special attention is paid to dimple edge resolution to reproduce the flow separation and shear layer gradients with a proper accuracy. The condition $y^+ \leq 1$ for the first grid point was satisfied even at the highest Reynolds number to ensure a correct estimation of the local heat flux. Validation for a spherical dimple package is presented in Fig. 3. Mean profiles of velocity and rms values for $\mathrm{Re}_H = 6521$ show a good agreement between experiment and simulation. At $\mathrm{Re}_H = 13042$ the rms values from LES are twice as high as experimental ones. Most probably the reason is the non sufficient accuracy of measurements at this Reynolds number. Indeed, for the smooth channel flow at

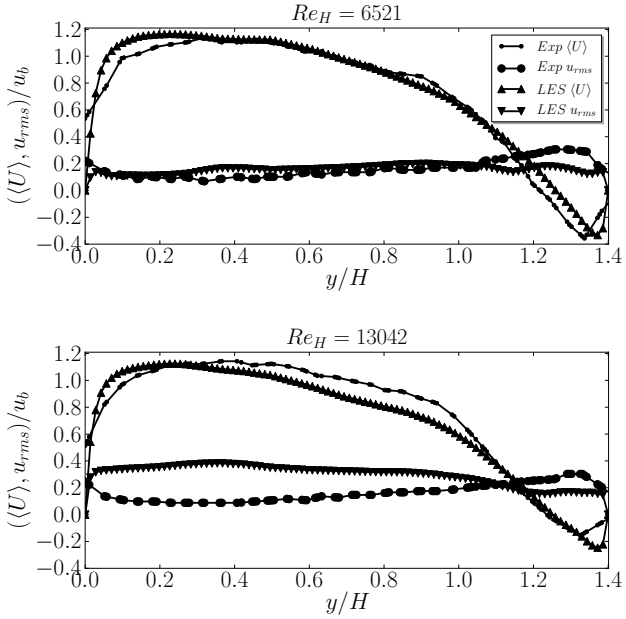

Figure 3: Velocity and rms profiles across the channel for dimples $t/D = 0.26$ at two different Reynolds numbers in the fully developed package flow. $y/H = 1.4$ is the dimple bottom

$\mathrm{Re}_H = 13042$ the rms values from LES reveal a high peak near the wall with a strong decrease towards the center of the channel. In contrast, the experimental rms values show no tendency to decrease far from the upper wall being nearly constant. Moreover, they decrease inside the dimple which normally acts as turbulence promoter.

Vortex structures

Various visualizations and numerical simulations of dimple packages show clearly that at small Reynolds numbers and shallow dimples the typical vortex structure is symmetric. For instance, visualizations using smoke wires performed by Ligrani P.M. (2003) at $\mathrm{Re}_H = 1250$ for dimples $t/D = 0.2$ revealed formation of one symmetric primary vortex pair in the center of the dimple and two secondary vortex pairs at each side in spanwise direction. It was reported that the formation of structures, ejection of fluid from the dimple and structures advection show periodic behaviour in streamwise direction.

At large Reynolds numbers commonly used vortex identification methods like λ_2 or Q criteria applied both for single dimple and dimple package reveal that the flow inside the cavities is dominated by small scale eddies. While for a single dimple it was possible to identify coherent structures by phase averaging (see Turnow J. (2010)), the flow on the dimple package is proved to be fully stochastic without any pronounced coherent structures. Any kind of order in vortex structures observed in a single dimple is destroyed in package due to irregular perturbations coming from dimples located upstream. However, some instantaneous cell patterns caused by dimples can be recognized in the streamline pictures averaged over $0.39s$ (see Figures 4 and 5). Analysis of pictures shows the mix of instantaneous symmetric and asymmetric structures. For instance, the streamline behaviour in the deep dimples (see Fig. 5) indicates the presence of an asymmetric vortex structure whereas the top dimple is filled with a symmetric one. Opposite flow topology in the top and the lowest dimples can be recognized in Figure 4. The flow topology is steadily changed in time showing no stable pattern where within the dimples it consists of many small scale eddies primarily arising in the shear layer shedding from the leading dimple edge. At the shedding point the vortices are nearly perpendicular to the local velocity vector, showing no stable preferential direction already at the place of their creation. Their further evolution is strongly influenced by interaction with irregular vortices coming from the dimples located upstream. One additional weighty argument in favour of absence of stable structures inclined to the incident flow is the nearly symmetric distribution of time averaged velocity profiles at $y/H = 0.9$ in transversal direction (see Figure 6). If any steady asymmetric structures exists as predicted from URANS calculations, the velocity distribution should be also asymmetric in experiments and LES within each dimple.

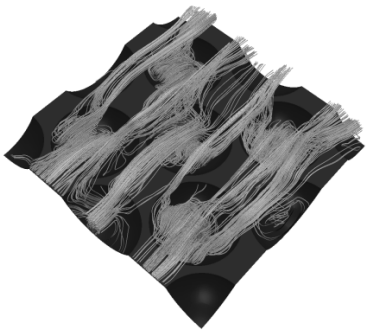

Figure 4: Time averaged streamlines at $t^+ = tU_b/L = 5$ for dimple package with the depth to diameter ratio of $t/D = 0.26$, $\mathrm{Re}_H = 13042$.

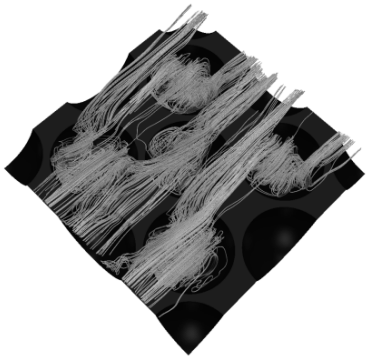

Figure 5: Time averaged streamlines at $t^+ = 5$ for dimple package with the depth to diameter ratio of $t/D = 0.326$, $\mathrm{Re}_H = 13042$.

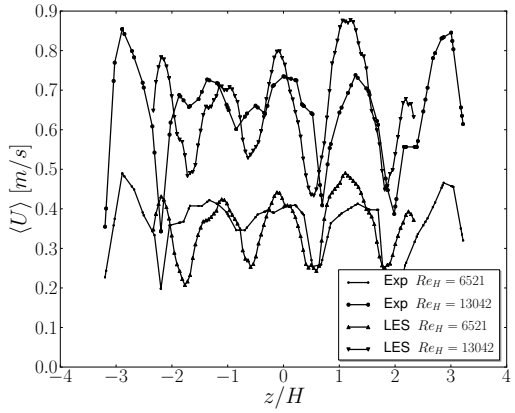

Figure 6: Time averaged velocity profiles at $y/H = 0.9$ in spanwise direction at $t/D = 0.26$ using LES method and experiment

Heat transfer

Table 3 illustrates the influence of the relative depth on hydraulic loss and heat transfer enhancement.

Table 3: Pressure resistance coefficient C_p and integral Nusselt number Nu for different dimple depths at $\mathrm{Re}_H = 6521$ and $\mathrm{Re}_H = 13042$.

	t/D	*0.195*	*0.26*	*0.315*
$\mathrm{Re}_H = 6521$	Nu/Nu_0	1.62	1.93	1.46
	C_p/C_{p0}	2.4	2.89	3.41
$\mathrm{Re}_H = 13042$	Nu/Nu_0	1.75	2.01	1.52
	C_p/C_{p0}	2.83	3.03	3.81

The integral Nusselt number $Nu/Nu_0 = 1.93$ at $\mathrm{Re}_H = 13042$ from LES agrees well with the value of $Nu/Nu_0 = 1.83$ given by Ligrani et al. at $\mathrm{Re}_H = 10200$ at $t/D = 0.22$. A significant discrepancy between LES and our measurements was documented for the pressure resistance coefficient C_p. Experimental pressure coefficient referred to the flat channel is $C_p/C_{p0} = 2.14$ at $\mathrm{Re}_H = 6521$ and $C_p/C_{p0} = 2.81$ at $\mathrm{Re}_H = 13042$ which is smaller than $C_p/C_{p0} = 2.89$ at $\mathrm{Re}_H = 6521$ and $C_p/C_{p0} = 3.03$ at $\mathrm{Re}_H = 13042$ obtained from numerical simulations.The most probable reason of this discrepancy is that the experimental dimple package has a finite length including a transitional section where the flow is far from the developed state. In LES the dimple package is treated as infinite one in all directions with full developed flow. That is why the pressure drop is sufficiently larger in simulations.

Calculation of the thermo- hydraulic performance $Nu/Nu_0/(C_p/C_{p0})^{1/3}$ shows the best results for dimples with the depth to diameter ratio of $t/D = 0.26$ what is in accordance with the expected one from literature survey. This result can be explained as follows. The flow inside the dimple is characterized by the strong reverse flow where the time averaged recirculation zone occupies nearly 80% of the whole cavity. The main flow separating from the leading edge reattaches at the windward side of the dimple and branches out. A part of the fluid is directly ejected back into the main flow producing vortex shedding at the downstream edge which results in a high level of mixing in the channel in front of the following dimple as predicted in the rms values in Figure 3. The highest rate of the heat transfer takes place within the reattachment zone where the cold flow is coming from the main flow. Inside the recirculation zone velocity is substantially decreased and thus the local heat fluxes are getting lower compared to a smooth channel. Additional enhancement of heat transfer is found due to variation of the reattachment line caused by shear layer fluctuations. The hot fluid is driven out of the dimple in transverse direction and leave the dimple on one or both dimple sides depending on the instantaneous flow topology (symmetric or asymmetric). Surprisingly, the outcoming fluid is not entering the following dimple as it might be expected, but due to its angle of outflow it moves directly into the main channel flow enhancing mixing process. The vortices arising in a dimple with $t/D = 0.26$ are stronger than these in the shallow dimple at $t/D = 0.195$. Therefore, both the hydraulic losses and the heat flux is increased (see Table 3). However, the further increase of the depth from $t/D = 0.26$ to $t/D = 0.326$ is followed by the heat exchange reduction. The reason for this phenomena can be explained by the decrease of the fluctuations caused by vortices of the shear layer when the dimple depth exceeds a certain threshold. The vortices generated in the shear layer over the dimple induce the fluctuations, driving the hot fluid from the surface and enhancing the mixing inside the dimple. The induced fluctuations depend both on the vortex intensity and on the ratio of the vortex scale to the dimple depth, i.e. on the distance between the dimple bottom and the vortex centres. In the case of $t/D = 0.26$ this ratio is sufficiently larger than in the case $t/D = 0.195$ whereas the vortex intensities are comparable. In deep dimples the recirculation zone is more stable. The hot fluid stays longer within the recirculation zone weakening the heat exchange. As a result, both the ratio Nu/Nu_0 and the thermo-hydraulic performance defined as $\frac{Nu}{Nu_0}/\frac{C_p}{C_{p0}}$ have a maximum at $t/D = 0.26$. Thus the optimal dimple should have a restricted depth to diameter ratio t/D. From one side, it can not be too small, because the creating vortices are not strong enough to enhance the mixing between the hot and cold fluid especially behind the dimple. From the other side, it can not be too large from two following reasons. First, the increase of t/D leads to a drastic decrease of the thermo-hydraulic performance, what is well known from previous investigations. Second, as shown in this paper, the heat exchange is getting worse when t/D exceeds a certain threshold, since the shear layer vortices are not able to provide efficient mixing in a large relatively stable recirculation zone.

PROPER ORTHOGONAL DECOMPOSITION

POD technique originally proposed by Lumley (1970) for turbulent flows is based on the Karhunen-Leòve decomposition for identification of spatial structures and estimation of their contributions to the total energy of the flow field. The decomposed fields are represented in the sum of products of space dependent functions $\Phi_i^{(n)}(\mathbf{x})$ and time dependent coefficients $a^{(n)}(t)$.

$$u_i(\mathbf{x},t) = \sum_{n=1}^{N} a^{(n)}(t)\Phi_i^{(n)}(\mathbf{x}) \tag{4}$$

For application of POD on vector fields the snapshot method proposed by L. (1987) is used for decomposition of the velocity field $\mathbf{u}(\mathbf{x},t)$ and pressure field $p(\mathbf{x},t)$. The turbulent fields $u_i(\mathbf{x},t)$ and $p(\mathbf{x},t)$ are taken from numerical calculations at equidistant time instants using 3500 samples at $\Delta t^+ = 0.0126$. The time averaged mean fields are subtracted from each field to consider only the fluctuations. In case of dimples, where the flow is dominated by eddies with a wide range of small scales, a rapid decay of the energy content within the first modes could not be observed. The first 190 modes represent about 49.95% of the total energy at $\mathrm{Re}_H = 13042$. Moreover, the energy of the first modes are nearly equal to each other for both investigated Reynolds numbers. Since the streamlines of the POD modes for $\mathrm{Re}_H = 6521$ look similarly to $\mathrm{Re}_H = 13042$ for dimples with a ratio of $t/D = 0.26$ only streamlines of the first mode of the velocity field $\Phi^{(1)}$ obtained for $\mathrm{Re}_H = 13042$ and $t/D = 0.26$ is presented in Figure 7. The

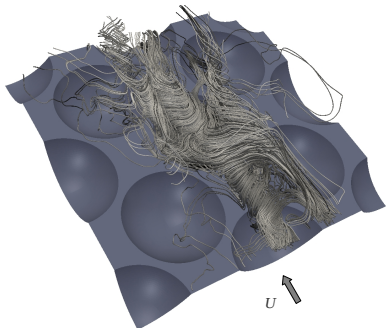

Figure 7: Streamlines of the first spatial mode $\Phi^{(1)}$ obtained from POD of the velocity field at $\mathrm{Re}_H = 13042$ for dimples with a ratio of $t/D = 0.26$.

first POD mode $\Phi^{(1)}$ reveals large rotating structures taking its origin inside the cavities and penetrating into the main channel flow. Topologically this structure is very similar to the tornado like structure proposed by Kiknadze from intuitive considerations at the beginning of the dimple developments in the late eighties. The first mode involves the fluid motion out of the dimple which results in a significant enhancement of the heat transfer. Furthermore, the mode axis is aligned with the main flow direction minimizing the pressure loss in heat exchanger channel. This is an additional explanation why the increase of the heat exchange in dimpled exchangers occurs at minimum hydraulic losses.

CONCLUSION

Experimental and numerical investigations have been performed for turbulent flow over spherical dimples in a staggered arrangement inside a narrow channel. It was shown that in contrast to the single dimple case, any coherent vortex structures are hardly to detect. The flow is chaotic and consists of small eddies with a broad range of scales. Snapshots of streamlines show some kind of cell pattern corresponding to dimple arrangement. The instantaneous flow within each dimple can have both symmetric and asymmetric forms for dimples at a ratio of $t/D = 0.26$. The forms are changed steadily in time revealing no stable configurations. Ejection of the heated fluid into the main channel flow occurs at the spanwise edges what is in accordance with visual observations of Ligrani P.M. (2003). The reason of the discrepancy between the flow topologies for a single dimple and dimpled package is the high level of perturbations coming into each dimple from dimples upstream. They prevent creation and evolution of large scale coherent structures. For both Reynolds numbers it was found that the dimple package with the depth t to diameter D ratio of $t/D = 0.26$ provides the highest heat transfer and thermo-hydraulic performance. At t/D smaller than 0.26 the vortices arising in the cavity are not strong enough to mix the hot and cold fluid effectively, what results in a weak heat transfer enhancement. When t/D is larger than 0.26 a relatively stable recirculation zone arises in the dimple. The vortices of the shear layer are not able to destroy the recirculation zone and hot fluid is kept longer in this zone weakening the heat flux. Proper Orthogonal Decomposition (POD) method is applied to resolved LES fields to identify spatial-temporal structures hidden in the random fluctuations of pressure and velocity fields. The first POD mode looks similar to tornado like structures proposed by Kiknadze from intuitive considerations. This structure with a strong inner rotation and large energy content is aligned with main flow direction.

ACKNOWLEDGMENT

This work was supported by the German Scientific Foundation (DFG). Numerical calculations have been performed at the High-Performance Computing center (HLRN) for northern Germany. We thank scientific group of Prof. Leder for their help in LDV measurements.

REFERENCES

L., Sirovich 1987 Turbulence and the dynamics of coherent structures. part i: coherent structures. part ii: symmetries and transformations. part iii: dynamics and scaling. *Quart. Appl. Math.* **45**, 561590.

Ligrani P.M., Oliveira M.M., Blaskovich T. 2003 Comparison of heat transfer augmentation techniques. *AIAA J.* **41** (3), 337–362.

Turnow J., Kornev N., Isaev S. Hassel E. 2010 Vortex mechanism of heat transfer enhancement in a channel with spherical and oval dimples. *Heat and Mass Transfer* **47** (3), 301–313.